First Observation of Electrorheological Plasmas

A. V. Ivlev,[1] G. E. Morfill,[1] H. M. Thomas,[1] C. Räth,[1] G. Joyce,[2] P. Huber,[1] R. Kompaneets,[1] V. E. Fortov,[3] A. M. Lipaev,[3] V. I. Molotkov,[3] T. Reiter,[4] M. Turin,[5] and P. Vinogradov[5]

[1]*Max-Planck-Institut für extraterrestrische Physik, 85741 Garching, Germany*
[2]*University of Maryland, College Park, Maryland 20742, USA*
[3]*Institute for High Energy Densities, Russian Academy of Sciences, 125412 Moscow, Russia*
[4]*European Astronaut Centre, 51147 Cologne, Germany*
[5]*RSC Energia, 141070 Korolev, Russia*

(Received 24 August 2007; published 6 March 2008)

We report the experimental discovery of "electrorheological (ER) complex plasmas," where the control of the interparticle interaction by an externally applied electric field is due to distortion of the Debye spheres that surround microparticles (dust) in a plasma. We show that interactions in ER plasmas under weak ac fields are mathematically equivalent to those in conventional ER fluids. Microgravity experiments, as well as molecular dynamics simulations, show a phase transition from an isotropic to an anisotropic (string) plasma state as the electric field is increased.

DOI: 10.1103/PhysRevLett.100.095003 PACS numbers: 52.27.Lw, 83.80.Gv

"Conventional" electrorheological (ER) fluids consist of suspensions of microparticles in (usually) nonconducting fluids with a different dielectric constant [1,2]. The interparticle interaction, and hence the rheology of ER fluids, is determined by an external electric field, which polarizes grains and thus induces additional dipole-dipole coupling. The electric field plays the role of a new degree of freedom that allows us to "tune" the interaction between particles. This makes the phase diagram of ER fluids remarkably diversified [3,4].

So far, colloidal suspensions have been the major focus for ER studies, providing a wealth of information [1–6]. The discovery that complex plasmas also have electrorheological properties adds a new dimension to such research—in terms of time or space scales and for studying new phenomena: Ensembles of microparticles in complex plasmas can act as an essentially single-species system with very weak damping [7]. This is very different from colloids [8] (it is a consequence of the fact that the neutral gas density in complex plasmas is $\sim 10^6$–10^8 times smaller than the fluid density in colloids). Therefore, complex ER plasmas cover new physics and enable us to investigate previously inaccessible rapid elementary processes that govern the dynamical behavior of ER fluids—at the level of individual particles. In particular, such investigations may allow us to study critical phenomena accompanying second-order phase transitions [9].

Laboratory complex plasmas are low-pressure gas-discharge plasmas containing monodisperse microparticles that are highly charged due to absorption of ambient electrons and ions [10,11]. Complex plasmas are charge-neutral and optically thin. In contrast to conventional ER fluids (e.g., colloids) where the induced dipoles are due to polarization of microparticles themselves, in complex plasmas the primary role is played by clouds of compensating plasma charges (mostly, excessive ions) surrounding negatively charged grains. A schematic illustration of the particle potential is shown in Fig. 1.

Quantitatively, the (field-induced) interparticle interaction in ER plasmas can be determined from the linearized dielectric response formalism based on the solution of the kinetic equations for the plasma species (the formalism is applicable as long as the perturbations of the ion density induced by a charged grain are weak at the relevant distances, see [11,12] for details). Such an approach allows us to calculate self-consistent wake potential as a function of the ion drift velocity. Without an electric field, the interaction is via the Debye-Hückel potential characterized by the particle charge Q and ion screening length λ. The external ac field E causes (mobility-limited) ion oscillations with the velocity $u_i = \mu_i E$, where $\mu_i \simeq 1.6 \times 10^5/p$ cm^2/(V s) for Ar ions in an Ar parent gas. Far-field asymptotics for the potential can be expanded into a series over (small) u_i (with the angular dependence of the first three coefficients of expansion being proportional to the corresponding multipoles, i.e., charge, dipole, quadrupole). Furthermore, *all* "odd" terms ($\propto u_i^j$ with odd j) are proportional to linear combinations of the odd-order Legendre polynomials, whereas "even" terms are combinations of the even-order polynomials. Thus, for an ac field $E(t)$ with $\langle E \rangle_t = 0$, all odd-order terms disappear in the time-averaged potential $\langle \phi \rangle_t$, which becomes an even function of coordinates. In spherical coordinates, the effective energy $Q\langle \phi \rangle_t$ of the time-averaged pair interaction is

$$W(r, \theta) \simeq Q^2 \left[\frac{e^{-r/\lambda}}{r} - 0.43 \frac{M_T^2 \lambda^2}{r^3} (3\cos^2\theta - 1) \right], \quad (1)$$

where θ is the angle between $\mathbf{E}$ and $\mathbf{r}$ and $M_T^2 = \langle u_i^2 \rangle_t / v_T^2$ is the (squared) "thermal" Mach number normalized by the thermal velocity of ions (equal to that of neutrals), $v_T^2 = T_n/m_i$ [12]. Thus, the interaction consists of two principal contributions: The first "core" term represents the spheri-

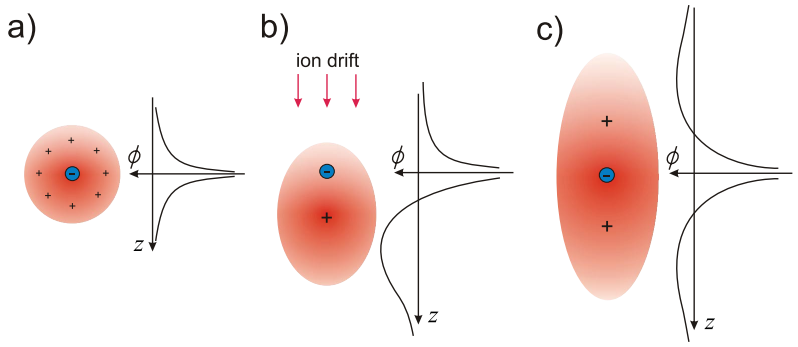

FIG. 1 (color). Particle potential in a complex plasma. The relevant (ion) screening length and, hence the effective radius of the polarizable cloud "attached" to a microparticle is typically 1-to-2 orders of magnitude larger than the particle size. Without an external field (a) the cloud is spherical (the so-called "Debye sphere"), when a field is applied (b) the cloud becomes asymmetric and acquires a fairly complicated shape. The "center" of the cloud—which is then called "ion wake"—is shifted downstream from the grain, along the field-induced ion drift. In this case the pair interaction between charged grains is generally nonreciprocal (i.e., non-Hamiltonian), because the wakes "belong" to the surrounding plasma and therefore play the role of a tenuous "third body" [19]. The nonreciprocity of the interaction could only be eliminated if the wake potential were an even function of coordinates, i.e., $\phi(\mathbf{r}) = \phi(-\mathbf{r})$. A simple "recipe" to create such a reciprocal wake potential is as follows: One has to apply an ac field of a frequency that is (i) much lower than the inverse time scale of the ion response (ion plasma frequency, typically $\sim 10^7$ s^{-1}) and, at the same time, (ii) much higher than the inverse dust response time (dust plasma frequency, typically $\sim 10^2$ s^{-1}). Then the ions react instantaneously to the field whereas the microparticles do not react at all. The effective interparticle interaction in this case is determined by the *time-averaged* wake potential (c). In the framework of the linear response formalism, the resulting interaction is rigorously reciprocal (Hamiltonian), so that one can directly apply the formalisms of statistical physics to describe ER plasmas.

cally symmetric Debye-Hückel (Yukawa) part, whereas the second term is due to the interaction between the charge of one grain and the quadrupole part of the wake produced by another grain. The charge-quadrupole interaction is identical to the interaction between two equal and parallel dipoles of magnitude $\simeq 0.65 M_T Q\lambda$—therefore we refer to the second term in Eq. (1) as the "dipole" term. This implies that for small M_T the interactions in ER plasmas are *equivalent* to dipolar interactions in conventional ER fluids.

The phase variables commonly used to describe ER colloids are the particle volume fraction and the electric field strength [3,4]. For ER plasmas, where the screening length is much larger than the particle size, the so-called "screening parameter" $\kappa = \Delta/\lambda$ is a more convenient phase variable (here and below $\Delta = n^{-1/3}$ is the mean interparticle distance), and the electric field can be measured in units of M_T. The core coupling is measured with the "coupling parameter" $\Gamma = Q^2/T\Delta$ [11].

Investigations of the phase states in ER colloids have largely concentrated on solids, because of the rich variety of possible crystalline states [1,3,4], whereas relatively little research of the fluid phase exists. In particular, the dynamics and details of the phase transition between isotropic and "string" fluids is still unexplored [13,14].

In order to quantify the expected "isotropic-to-string" phase transition, a suitable order parameter has to be employed that is sensitive to the changing particle structures. Conventional approaches, e.g., binary correlation or bond orientation functions, Legendre polynomials, etc., were too insensitive in our case. A much more satisfactory order parameter is the anisotropic scaling index α—a local nonlinear measure for structure characterization (for details, see, e.g., [15]), with which any symmetry changes can be quantified by using "principal axes" distributions: $P_x(\alpha)$, $P_y(\alpha)$, and $P_z(\alpha)$, where $P_{\mathbf{q}}(\alpha)d\alpha = \mathrm{P}\{\alpha \in [\alpha, \alpha + d\alpha[, \mathbf{q}\}$. The emergence of anisotropic structures is reflected by decreasing α for particular direction $\mathbf{q}$. In our case the problem has uniaxial anisotropy (field is in the z direction), so that $P_x(\alpha)$ and $P_y(\alpha)$ are statistically the same. Therefore, longitudinal and transverse distributions defined as $P_{\parallel}(\alpha) \equiv P_z(\alpha)$ and $P_{\perp}(\alpha) \equiv \frac{1}{2}[P_x(\alpha) + P_y(\alpha)]$ are employed below.

The MD simulations [16] of a weakly coupled ER plasma (using 45 000 particles) were performed for different combinations of κ and Γ that ensure sufficiently small magnitude of the pair interaction energy, viz., $\Gamma e^{-\kappa} \lesssim 1$. We found that at sufficiently small M_T the distributions $P_{\parallel}$ and $P_{\perp}$ practically coincide. This suggests an isotropic and homogeneous distribution of particles, unaffected by the electric field. At larger M_T the transverse distribution remains practically unchanged, whereas the longitudinal distribution is noticeably shifted towards smaller α. This is an indicator for the emergence of stringlike patterns along the field—for aligned 1D structures the scaling index should decrease towards unity [15].

A quite natural (and simple) scalar order parameter to characterize the onset of the isotropic-to-string transition is the difference between the transverse and longitudinal scaling indices averaged over the ensemble, $\Delta\alpha = \int \alpha P_{\perp} d\alpha - \int \alpha P_{\parallel} d\alpha$. Figure 2 summarizes the simulation results for $\Gamma e^{-\kappa} \simeq 0.24$ (orange or light gray bullets

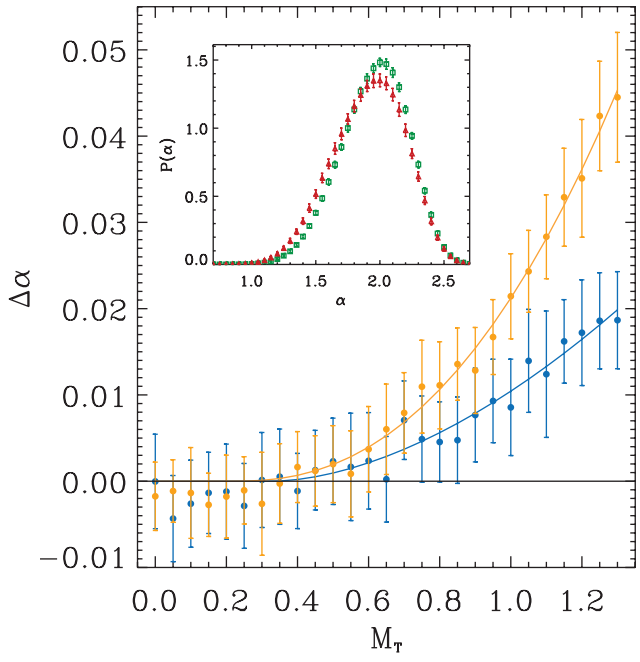

FIG. 2 (color). Onset of the isotropic-to-string plasma transition. Order parameter $\Delta\alpha$ (average difference of transverse and longitudinal scaling indices) versus control parameter M_T (thermal Mach number of the ion oscillations) is obtained from MD simulations for two cases of weakly coupled ER plasmas: coupling parameter $\Gamma = 530$ (orange bullets) and $\Gamma = 133$ (blue bullets), screening parameter $\kappa = 7.7$ for both cases. A two-parametric least-squares fit $\Delta\alpha \propto (M_T - M_T^{\rm cr})^\beta$ for $M_T > M_T^{\rm cr}$ and $\Delta\alpha = 0$ for $M_T \le M_T^{\rm cr}$ yields $M_T^{\rm cr} = 0.22$ and $\beta = 2.3$ (orange line), and $M_T^{\rm cr} = 0.33$ and $\beta = 1.7$ (blue line). The inset shows an example of histograms for longitudinal (red triangles) and transverse (green squares) distributions of the scaling indices, $P_\parallel(\alpha)$ and $P_\perp(\alpha)$, calculated for $\Gamma = 530$ at $M_T = 1.3$. Note that a uniform and isotropic set of points makes $P(\alpha)$ peaked at $\alpha \simeq 1.9$.

and line) and $\Gamma e^{-\kappa} \simeq 0.06$ (blue or gray bullets and line). The calculated values of the order parameter $\Delta\alpha$ versus the control parameter M_T are fitted by power-law functions. The fit yields an offset $M_T^{\rm cr}$—a measure of the critical field—of 0.22 and 0.33, respectively. Note that if we were to enforce $M_T^{\rm cr} = 0$, we would obtain unreasonably high values of the chi-square parameter (~10 larger than those for the curves shown in Fig. 2), which strongly suggests that we have a second-order or a weak first-order phase transition between isotropic and string fluids.

We can make a simple analytical estimate for the thermodynamic stability of weakly coupled ER plasmas and derive a rough criterion for the isotropic-to-string phase transition: Weak coupling implies a rarefied (gaseous) ensemble of particles, where triple interactions play a minor role. Thermodynamic properties of such systems can be understood in terms of the second virial coefficient [17]: $B = \pi \int_0^\infty \int_{-1}^1 (1 - e^{-\tilde{W}}) r^2 dr dx$, where $x = \cos\theta$ and $\tilde{W}(r, x) = W/T$. The core interaction radius in Eq. (1) (radius of excluded volume, in units of λ) is approximated by $\tilde{R}_{\rm ex} \sim \ln(\Gamma\kappa) \gg 1$ (for typical experiments $\Gamma \sim 10^3$–10^5 and $\kappa \sim 1$–10). For $M_T^2 \lesssim \tilde{R}_{\rm ex}^3/(\Gamma\kappa)$ the integration yields the following estimate: $(\pi\lambda^3)^{-1} B \simeq \frac{2}{3}\tilde{R}_{\rm ex}^3 - 0.04(\Gamma\kappa M_T^2)^2/\tilde{R}_{\rm ex}^3$. At larger Mach numbers the attractive interaction provides an exponentially large contribution to B and, hence, the virial coefficient rapidly becomes negative. Thermodynamic stability requires $2nB \gtrsim -1$ [17], and the violation of this condition suggests the occurrence of a phase transition to a string fluid. This happens when $M_T^2 \gtrsim 3\sqrt{1 + N_{\rm ex}^{-1}}\tilde{R}_{\rm ex}^3/(\Gamma\kappa)$, where $N_{\rm ex} = \frac{4}{3}\pi R_{\rm ex}^3 n \lesssim 1$ is the number of particles per excluded volume. For the MD simulations shown in Fig. 2 this simple estimate gives critical values $M_T^{\rm cr} \simeq 0.4$ (blue line) and $\simeq 0.6$ (red line)—a good agreement for such an "order-of-magnitude" evaluation.

Experiments with ER plasmas were performed with the "PK-3 Plus" laboratory [18] under microgravity conditions, on board of the International Space Station (ISS). We used microparticles of different sizes (diameters ≃1.55 μm, 6.8 μm, and 14.9 μm), and Ar gas at pressures between 8 and 15 Pa. To ensure different number densities n, the number of injected particles varied as well. Sinusoidal out-of-phase signals were applied to the rf electrodes at frequency 100 Hz, with the peak-to-peak voltage between 26.6 and 65.6 V varied in steps of 2.2 V. In each experiment an ac field was first ramped up, and then ramped down. At weak fields charged particles form a strongly coupled ($\Gamma e^{-\kappa} \sim$ 30–100) isotropic fluid phase with typical short-range order. As the field is increased above a certain threshold, particles start to rearrange themselves and become more and more ordered, until eventually well-defined particle strings are formed. The transition between isotropic and string fluid states is fully reversible—decreasing the field brings the particles back into their initial isotropic state. The trend to form strings increases with particle size, which is in line with our above theoretical estimates. However, the quantitative comparisons with the estimates are meaningless due to the rather strong coupling and, hence, multiple particle correlations. On the other hand, the MD simulations performed with similar parameters demonstrate remarkable agreement with the experiment.

Figure 3 shows the experimental results with 6.8 μm particles at $p = 10$ Pa and the comparison with the MD simulations. (Parameters of the experiment are estimated as follows: $\lambda \simeq 0.05$ mm, $n \simeq 3 \times 10^4$ cm^{-3}, $Q \simeq -10^4 e$, and $T \simeq 3 \times 10^{-2}$ eV.) The structural order of the well-developed strings is quite evident in both experimental and simulation data shown in the first two rows. The lower two rows show the corresponding distributions $P_\parallel(\alpha)$ and $P_\perp(\alpha)$. As the electric field is increased, $P_\perp$ remains practically unchanged whereas $P_\parallel$ is shifted towards $\alpha \simeq 1$, suggesting strong 1D ordering (strings). Note that the local amplitude of the electric field in the experiment cannot be measured or directly calculated, due to unknown plasma screening. However, from the comparison with the MD simulations one can deduce the corresponding M_T

3×10^4 cm^{-3}

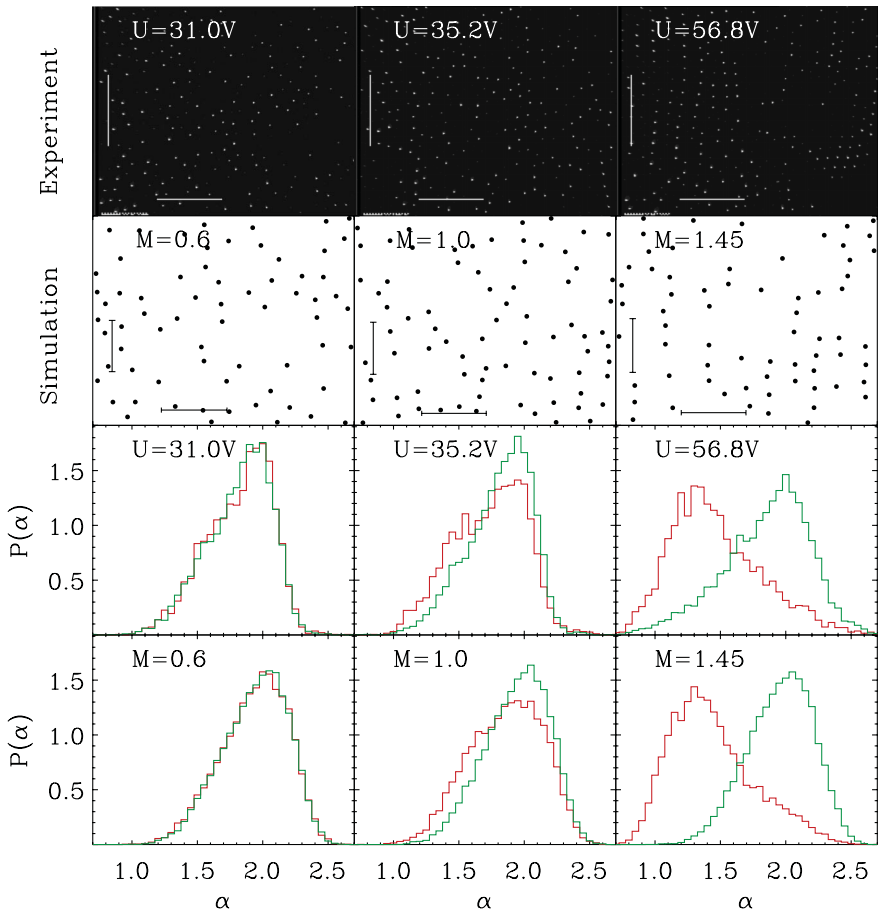

FIG. 3 (color). Formation of developed strings in ER plasmas. First row: Microgravity experiments (6.8 μm particles, raw data), microparticles are illuminated by a thin (less than mean interparticle distance) laser sheet parallel to the applied ac electric field. Examples of "low" (first column), "intermediate" (second column), and "high" (third column) fields are shown, the peak-to-peak voltage of the ac signal (applied to two parallel horizontal electrodes) is indicated. Second row: MD simulations, the same configuration, field is measured in units of the thermal Mach number M_T (scale bars 2 mm). Third and forth rows: Histograms for longitudinal (red) and transverse (green) distributions of the scaling indices, $P_{\|}(\alpha)$ and $P_{\perp}(\alpha)$, calculated for the experiment and simulation, respectively. (Note that at higher densities the particle positions in the neighboring strings became highly correlated.)

and, hence, the effective magnitude of the field, which turns out to be a factor ~3–10 smaller than the "vacuum" value U/H (here U is the ac peak-to-peak voltage at the electrodes and H is the distance between them).

Complex plasmas enable us to study elementary dynamical processes by observing the fully resolved motion of individual particles, and we expect that future ER plasma investigations will make ample use of these unique properties. Such studies should provide us with essential knowledge about generic phenomena that govern the behavior of ER fluids in general.

This work was supported by DLR/BMWi Grant No. 50WP0203, and by RFBR Grant No. 06-02-08100. We would like to thank the firm Kayser-Threde, RKK-Energia, the Mission Control Centre in Korolev, and, finally, the Yuri Gagarin Cosmonaut Training Centre and the cosmonauts for their perfect work.

[1] T. Chen, R. N. Zitter, and R. Tao, Phys. Rev. Lett. **68**, 2555 (1992).
[2] U. Dassanayake, S. Fraden, and A. van Blaaderen, J. Chem. Phys. **112**, 3851 (2000).
[3] A. Yethiraj and A. van Blaaderen, Nature (London) **421**, 513 (2003).
[4] A.-P. Hynninen and M. Dijkstra, Phys. Rev. Lett. **94**, 138303 (2005).
[5] J. E. Martin, J. Odinek, and T. C. Halsey, Phys. Rev. Lett. **69**, 1524 (1992).
[6] M. Parthasarathy and D. J. Klindenberg, Mater. Sci. Eng., R **17**, 57 (1996).
[7] S. A. Khrapak, A. V. Ivlev, and G. E. Morfill, Phys. Rev. E **70**, 056405 (2004).
[8] V. J. Anderson and H. N. W. Lekkerkerker, Nature (London) **416**, 811 (2002).
[9] S. A. Khrapak *et al.*, Phys. Rev. Lett. **96**, 015001 (2006).
[10] P. K. Shukla and A. A. Mamun, *Introduction to Dusty Plasma Physics* (IOP, Bristol, 2002).
[11] V. E. Fortov *et al.*, Phys. Rep. **421**, 1 (2005).
[12] R. Kompaneets, Ph.D. thesis, Ludwig-Maximilians-Universität München, 2007, available at http://edoc.ub.uni-muenchen.de/7380.
[13] R. Tao, Phys. Rev. E **47**, 423 (1993).
[14] G. L. Gulley and R. Tao, Phys. Rev. E **56**, 4328 (1997).
[15] C. Räth *et al.*, Mon. Not. R. Astron. Soc. **337**, 413 (2002).
[16] G. Joyce, M. Lampe, and G. Ganguli, in *Space Plasma Simulation*, edited by J. Buechner, C. T. Dum, and M. Scholer (Springer, Berlin, 2003), p. 125.
[17] L. D. Landau and E. M. Lifshitz, *Statistical Physics* (Pergamon, Oxford, 1978), Part I.
[18] H. M. Thomas *et al.*, "Complex Plasma Laboratory PK-3 Plus on the International Space Station," New J. Phys. (to be published).
[19] A. Melzer, V. A. Schweigert, and A. Piel, Phys. Rev. Lett. **83**, 3194 (1999).